The Five Lagrange Points: PARKING PLACES IN SPACE

Part II: Mechanical Stability at Lagrange Points

by Dwight E. Neuenschwander, Southern Nazarene University, Emeritus

In Part I of this article, published in the Fall 2023 issue of *Radiations*, we explore finding Lagrange points. Now we continue this discussion by moving on to the mechanical stability at Lagrange points. You may recall that a Lagrange point is a location in the vicinity of a gravitationally bound, two-body system where a small object, such as a satellite, maintains a stationary position relative to the major bodies. The James Webb Space Telescope (JWST) is located at Lagrange point L2 in the Sun-Earth system. Figures 1 and 2 are repeated from Part I below.

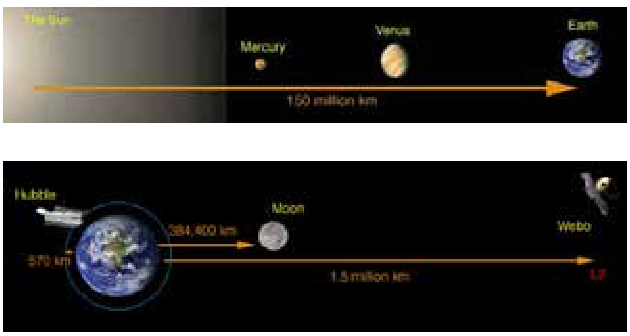

Figure 1. Top: Distance between the Sun and Earth. Bottom: JWST (the Webb) orbits the Sun 1.5 million kilometers away from the Earth at what is called the second Lagrange point or L2. Credit: NASA.

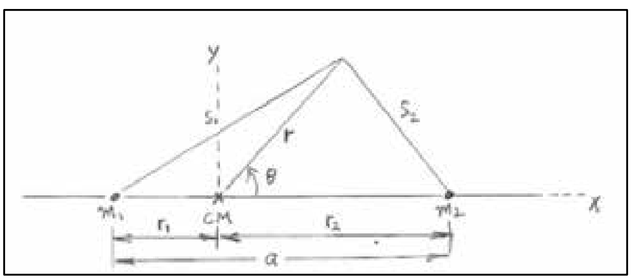

Figure 2. The coordinate system used to find Lagrange points.

Criteria for Stability

The Lagrange points offer sites of mechanical equilibrium to satellites or asteroids stationed there. Are these locations points of stable equilibrium—or are they unstable? To approach this issue requires an examination of the second derivatives of $\varphi_\omega(x, y)$. From Eq. (24) of Part I,

$$\varphi_\omega(r, \theta) = -\frac{Gm_1}{s_1} - \frac{Gm_2}{s_2} - \frac{1}{2}(x^2 + y^2)\omega^2 , \tag{41}$$

where, according to Fig. 2,

$$s_1 = [(x + r_1)^2 + y^2]^{1/2} \tag{42}$$

and

$$s_2 = [(r_2 - x)^2 + y^2]^{1/2}. \tag{43}$$

With respect to x the second derivative reads

$$\frac{\partial^2 \varphi_\omega}{\partial x^2} = -\frac{2Gm_1}{s_1^3}\left(\frac{\partial s_1}{\partial x}\right)^2 + \frac{Gm_1}{s_1^2}\left(\frac{\partial^2 s_1}{\partial x^2}\right) - \frac{2Gm_2}{s_2^3}\left(\frac{\partial s_2}{\partial x}\right)^2 + \frac{Gm_2}{s_2^2}\left(\frac{\partial^2 s_2}{\partial x^2}\right) - \omega^2. \tag{44}$$

Using Eqs. (42) and (43) to evaluate the derivatives of s_1 and s_2 turns Eq. (44) into

$$\frac{\partial^2 \varphi_\omega}{\partial x^2} = -\frac{2Gm_1}{s_1^3}\left(\frac{x + r_1}{s_1}\right)^2 - \frac{2Gm_2}{s_2^3}\left(\frac{x - r_2}{s_2}\right)^2 - \omega^2 + \frac{Gm_1}{s_1^3}\left[-\left(\frac{x + r_1}{s_1}\right)^2 + 1\right] + \frac{Gm_2}{s_2^3}\left[-\left(\frac{x - r_2}{s_2}\right)^2 + 1\right]. \tag{45}$$

By similar reasoning we find

$$\frac{\partial^2\varphi_\omega}{\partial y^2} = -\frac{2Gm_1}{s_1^3}\left(\frac{y}{s_1}\right)^2 - \frac{2Gm_2}{s_2^3}\left(\frac{y}{s_2}\right)^2 - \omega^2$$

$$+\frac{Gm_1}{s_1^3}\left[-\left(\frac{y}{s_1}\right)^2 + 1\right] + \frac{Gm_2}{s_2^3}\left[-\left(\frac{y}{s_2}\right)^2 + 1\right], \quad (46)$$

and recalling that the second derivatives commute, so that $\partial^2\varphi_\omega/\partial x\partial y = \partial^2\varphi_\omega/\partial y\partial x$,

$$\frac{\partial^2\varphi_\omega}{\partial y\partial x} = -\frac{3Gm_1}{s_1^3}\left(\frac{x+r_1}{s_1}\right)\left(\frac{y}{s_1}\right) - \frac{3Gm_2}{s_2^3}\left(\frac{x-r_2}{s_2}\right)\left(\frac{y}{s_2}\right). \quad (47)$$

In pursuing the inferences of Eqs. (45–46), recall Eq. (14), $\omega^2 = GM/a^3$.

At the Lagrange points L4 and L5, $s_1 = s_2 = a$; $(x+r_1)/a = (r_2-x)/a = \cos 60^\circ = 1/2$; and $y/a = \sin 60^\circ = \sqrt{3}/2$. Here Eqs. (45)–(47) yield, respectively,[7]

$$\left[\frac{\partial^2\varphi_\omega}{\partial x^2}\right]_{L4,\ L5} = -\frac{3}{4}\frac{GM}{a^3}, \quad (48)$$

$$\left[\frac{\partial^2\varphi_\omega}{\partial y^2}\right]_{L4,\ L5} = -\frac{9}{4}\frac{GM}{a^3}, \quad (49)$$

and

$$\left[\frac{\partial^2\varphi_\omega}{\partial y\partial x}\right]_{L4,\ L5} = -\frac{\sqrt{27}}{4}\frac{GM\kappa}{a^3}, \quad (50)$$

where $\kappa \equiv (m_1 - m_2)/M$. Since all of these second derivatives are never positive, L4 and L5 are "summits" in the effective potential φ_ω, locations of unstable equilibrium.

Turning to L1, L2, and L3, from Fig. 2, here are the values of s_1 and s_2 at these locations:

$s_1 = x + r_1$ at L1 and L2, $s_1 = |x| - r_1 = -(x + r_1)$ at L3;

$s_2 = r_2 - x$ at L1, $s_2 = x - r_2$ at L2, $s_2 = r_2 + |x| = r_2 - x$ at L3.

With these relations, and since $y = 0$ along the x-axis, the second derivatives of the effective potential for L1, L2, and L3 appear quite compact:

$$\left[\frac{\partial^2\varphi_\omega}{\partial x^2}\right]_{L1-L3} = -2G\left(\frac{m_1}{s_1^3} + \frac{m_2}{s_2^3}\right) - \frac{GM}{a^2}, \quad (51a)$$

$$\left[\frac{\partial^2\varphi_\omega}{\partial y^2}\right]_{L1-L3} = G\left(\frac{m_1}{s_1^3} + \frac{m_2}{s_2^3}\right) - \frac{GM}{a^2}, \quad (51b)$$

and

$$\left[\frac{\partial^2\varphi_\omega}{\partial y\partial x}\right]_{L1-L3} = 0. \quad (51c)$$

Recall Eq. (40a-c) from Part I:

$$L1: \quad r \approx a\left[1 - \left(\frac{\alpha}{3}\right)^{1/3}\right] \quad (40a)$$

$$L2: \quad r \approx a\left[1 + \left(\frac{\alpha}{3}\right)^{1/3}\right] \quad (40b)$$

$$L3: \quad r \approx a\left[1 + \frac{\alpha}{3}\right]. \quad (40c)$$

The various values of r in Eq. (40) are the values of $|x|$ in Eqs. (51a) – (51c). For the Sun–Earth system, $m_1 \approx 2\times 10^{30}$ kg, $m_2 \approx 6\times 10^{24}$ kg, $a \approx 1.5\times 10^{11}$ m. Using Eqs. (31), (32), and (40), along with the approximations that led to Eq. (40), when working out estimates for s_1 and s_2 for L1, we obtain[8]

$$\left[\frac{\partial^2\varphi_\omega}{\partial x^2}\right]_{L1,\ Sun-Earth} \approx -10\omega^2, \quad (52)$$

$$\left[\frac{\partial^2\varphi_\omega}{\partial y^2}\right]_{L1,\ Sun-Earth} \approx 3\omega^2, \quad (53)$$

where $\omega = 2\pi$ rad/yr. A plot of $\varphi_\omega(x, y)$ (Fig. 4) shows the neighborhood of L1 to be a saddle surface—displacements in the y direction are subject to a restoring force, but displacements in x direction encounter a repulsive force. By a similar analysis, the neighborhoods of L2 and L3 are saddle surfaces. Figure 4 shows the contours in the xy plane slice of φ_ω equipotential surfaces.

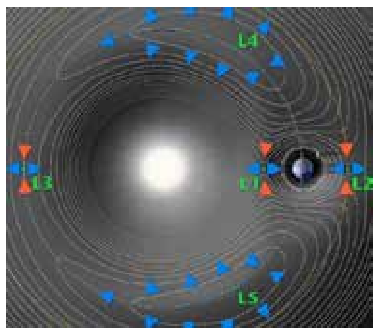

Figure 4. *Equipotential surfaces in the xy plane for φ_ω and the Roche lobe. Photo credit: NASA.*

Near a star in a binary system the equipotential surfaces are essentially spheres centered on the star. But the centrifugal potential stretches the equipotential surfaces between the stars into a shape resembling a toy balloon. L1 is located at the narrow end of the "balloon." The volume within the "balloon" that includes L1 is called the Roche lobe. If the star's outer layers extend beyond the Roche lobe, that matter "slides" over the "saddle" onto the companion star. This phenomenon drives Type 1a supernovas in a star-white dwarf binary system. When the white dwarf grabs enough mass from the companion to exceed the Chandrasekhar limit (~1.4$M_{\odot}$), the white dwarf explodes.

We have seen that at all five Lagrange points, the second derivatives of φ_ω are either negative for displacements in orthogonal directions, or describe saddle points. If this was the end of the story, a small body placed at a Lagrange point, when nudged off to one side, would be driven away from the region. The James Webb and other telescopes that are or have been parked at L2 must undergo small but frequent corrective maneuvers, like balancing a long pole vertically on the end of your nose. But that is not the entire story. Once the test particle of mass m' begins sliding off the Lagrange point, it acquires a nonzero velocity **v** and the Coriolis force kicks in. When that happens, as long as the gravitational and centrifugal forces still essentially cancel, Eq. (15)—Newton's second law transformed to a rotating reference frame—is roughly

$$-2m'(\boldsymbol{\omega} \times \mathbf{v}) \approx m'\mathbf{a}. \qquad (54)$$

For simplicity, consider **v** to be in the xy plane and recall that $\boldsymbol{\omega} = \omega\hat{\mathbf{k}}$. A moment's reflection on the direction of the cross product $-(\boldsymbol{\omega} \times \mathbf{v})$ shows that m' will move in a circular orbit around the Lagrange point at some radius R, so that from Eqs. (15) and (54),

$$2\omega v \approx \frac{v^2}{R}\,. \qquad (55)$$

Using $v = R\omega'$ for the orbital angular velocity ω' of m' around the Lagrange point, this results in $\omega' = 2\omega$. This quantitative result must not be taken too seriously, but it is qualitatively suggestive. Let's return to Eq. (15) and do a more thorough job with the Coriolis force included.

Turning on the Coriolis Force

For this discussion let $\mathbf{r}_o$ denote the location of a Lagrange point relative to the center of mass, and consider a small displacement $\boldsymbol{\varepsilon}$ from it to a nearby position $\mathbf{r}$, so that

$$\mathbf{r} = \mathbf{r}_o + \boldsymbol{\varepsilon}\,, \qquad (56)$$

where $|\boldsymbol{\varepsilon}| \ll r_o$. Write the αth component of Eq. (15) to first order in ε. We need the Taylor series expansion of $\mathbf{g}$ about $\boldsymbol{\varepsilon} = \mathbf{0}$. With repeated indices denoting summations (α, β subscripts denote x or y components) we obtain

$$\mathrm{g}_\alpha(\mathbf{r}) = \mathrm{g}_\alpha(\mathbf{r}_o) + \varepsilon_\beta \left[\frac{\partial \mathrm{g}_\alpha}{\partial x_\beta}\right]_{\mathbf{0}} + \cdots$$

$$= \mathrm{g}_\alpha(\mathbf{r}_o) - \varepsilon_\beta \left[\frac{\partial^2 \varphi}{\partial x_\beta \partial x_\alpha}\right]_{\mathbf{0}} + \cdots. \qquad (57)$$

Notice that Eq. (57) takes derivatives of the gravitational potential φ only (not φ_ω). Now to first order in $\boldsymbol{\varepsilon}$ the αth component of Eq. (15) is

$$\mathrm{g}_\alpha(\mathbf{r}_o) - \varepsilon_\beta \left[\frac{\partial^2 \varphi}{\partial x_\beta \partial x_\alpha}\right]_{\mathbf{0}} - 2(\boldsymbol{\omega} \times \dot{\boldsymbol{\varepsilon}})_\alpha - \{\boldsymbol{\omega} \times [\boldsymbol{\omega} \times (\mathbf{r}_o + \boldsymbol{\varepsilon})]\}_\alpha = \ddot{\varepsilon}_\alpha\,, \qquad (58)$$

where dots denote time derivatives. Recalling that $\mathbf{g}(\mathbf{r}_o) - \boldsymbol{\omega} \times (\boldsymbol{\omega} \times \mathbf{r}_o) = \mathbf{0}$ locates a Lagrange point, for x we are left with

$$-\varepsilon_x \left[\frac{\partial^2 \varphi}{\partial x^2}\right]_{\mathbf{0}} - \varepsilon_y \left[\frac{\partial^2 \varphi}{\partial y \partial x}\right]_{\mathbf{0}} - 2(\boldsymbol{\omega} \times \dot{\boldsymbol{\varepsilon}})_x - [\boldsymbol{\omega} \times (\boldsymbol{\omega} \times \boldsymbol{\varepsilon})]_x = \ddot{\varepsilon}_x \qquad (59)$$

and for y

$$-\varepsilon_x \left[\frac{\partial^2 \varphi}{\partial y \partial x}\right]_{\mathbf{0}} - \varepsilon_y \left[\frac{\partial^2 \varphi}{\partial y^2}\right]_{\mathbf{0}} - 2(\boldsymbol{\omega} \times \dot{\boldsymbol{\varepsilon}})_y - [\boldsymbol{\omega} \times (\boldsymbol{\omega} \times \boldsymbol{\varepsilon})]_y = \ddot{\varepsilon}_y. \qquad (60)$$

In particular, with $\boldsymbol{\omega} = \omega\hat{\mathbf{k}}$,

$$\boldsymbol{\omega} \times \dot{\boldsymbol{\varepsilon}} = \begin{vmatrix} \hat{\mathbf{i}} & \hat{\mathbf{j}} & \hat{\mathbf{k}} \\ 0 & 0 & \omega \\ \dot{\varepsilon}_x & \dot{\varepsilon}_y & 0 \end{vmatrix} = \omega\left(-\hat{\mathbf{i}}\dot{\varepsilon}_y + \hat{\mathbf{j}}\dot{\varepsilon}_x\right) \qquad (61)$$

and

$$\boldsymbol{\omega} \times (\boldsymbol{\omega} \times \boldsymbol{\varepsilon}) = -\omega^2 \boldsymbol{\varepsilon}\,. \qquad (62)$$

Recalling that $\varphi_\omega = \varphi - r^2\omega^2/2$, Eqs. (59) and (60) respectively become

$$-\varepsilon_x \left[\frac{\partial^2 \varphi_\omega}{\partial x^2}\right]_{\mathbf{0}} - \varepsilon_y \left[\frac{\partial^2 \varphi_\omega}{\partial y \partial x}\right]_{\mathbf{0}} + 2\omega\dot{\varepsilon}_y = \ddot{\varepsilon}_x \qquad (63)$$

and

$$-\varepsilon_x \left[\frac{\partial^2 \varphi_\omega}{\partial y \partial x}\right]_{\mathbf{0}} - \varepsilon_y \left[\frac{\partial^2 \varphi_\omega}{\partial y^2}\right]_{\mathbf{0}} - 2\omega\dot{\varepsilon}_x = \ddot{\varepsilon}_y. \qquad (64)$$

Again, let's get a feel for the system's possible behavior by considering two oversimplified but suggestive special cases:

1. If the second derivatives of φ_ω conveniently vanished, Eqs. (63) and (64) would reinforce the notion that a particle displaced gently off a Lagrange point would orbit that point. To see this, temporarily set the second derivatives of φ_ω in Eqs. (63) and (64) equal to zero, multiply Eq. (64) by $i = \sqrt{-1}$, and then add the two equations. Let $z = \varepsilon_x + i\varepsilon_y$, which leads to $\ddot{z} + 2i\omega\dot{z} - \omega^2 z = 0$, with solution $z(t) = Re^{-i\omega t}$, where R = const. Then $\varepsilon_x = (z + z^*)/2 = R\cos(\omega t)$ (where * denotes complex conjugate) and $\varepsilon_y = (z - z^*)/2i = -R\sin(\omega t)$. These results indicate a circular orbit of radius R with the particle moving in the opposite sense of the two-body system's rotation.

2. If the velocity terms were also absent, Eqs. (63) and (64) would produce $\ddot{z} - \omega^2 z = 0$, so ε_x and ε_y would mathematically go as $e^{\pm\omega t}$. But coming off a point of unstable equilibrium, we expect the physical solution to go as $e^{+\omega t}$, driving a particle away from the Lagrange point.

But again, these are merely suggestive, intuition-building, special-case musings. The dynamics includes all the terms in Eqs. (63) and (64), and we must deal with them. They are coupled in a way that does not allow a tidy separation trick like the one with z. Another approach is needed.

Lagrange Points as an Eigenvalue Problem

To save typographical space in what follows, denote $[\partial^2\varphi_\omega/\partial x^2]_{\mathbf{0}} \equiv \varphi_{\omega_{xx}}$ and similarly for the other second derivatives. Let's write Eqs. (63) and (64) as a matrix equation:

$$\begin{pmatrix} -\varphi_{\omega_{xx}} & -\varphi_{\omega_{yx}} & 0 & 2\omega \\ -\varphi_{\omega_{yx}} & -\varphi_{\omega_{yy}} & -2\omega & 0 \\ 0 & 0 & 1 & 0 \\ 0 & 0 & 0 & 1 \end{pmatrix} \begin{pmatrix} \varepsilon_x \\ \varepsilon_y \\ \dot{\varepsilon}_x \\ \dot{\varepsilon}_y \end{pmatrix} = \frac{d}{dt} \begin{pmatrix} \dot{\varepsilon}_x \\ \dot{\varepsilon}_y \\ \varepsilon_x \\ \varepsilon_y \end{pmatrix}. \quad (65)$$

The information in the column matrix $\begin{pmatrix} \boldsymbol{\varepsilon} \\ \dot{\boldsymbol{\varepsilon}} \end{pmatrix}$ describes the instantaneous state of a particle in four-dimensional "phase space"[9] when its location and velocity lie in the xy plane. For the moment, let's give the 4×4 matrix in Eq. (65) the name Λ. One way to approach Eqs. (63) and (64) is to find the eigenvalues of Λ. To find them and their corresponding eigenvectors is to find a set of basis vectors in the phase space, a set of vectors in terms of which any vector in the space can be written by their superposition.[10] Suppose you have some vector $|x>$ (written as a column matrix) operated on by a square matrix Γ to give a new vector $\Gamma|x>$. If $|x>$ happens to be an eigenvector of Γ, then Γ merely rescales $|x>$ but does not rotate it, so that $\Gamma|x> = \mu|x>$, where $\mu = const$. In other words, $(\Gamma - \mu 1)|x> = |0>$, where 1 in this context denotes the unit matrix and $|0>$ the zero vector. The invertible matrix theorem[11] says a nontrivial (but not unique) solution exists only if the determinant $|\Gamma - \mu 1| = 0$. This offers an equation to solve for the eigenvalues. Once they are found, within an overall factor each eigenvector corresponding to its eigenvalue follows by equating vector components on both sides of $\Gamma|x> = \mu|x>$. We apply this strategy to Eq. (65).

However, Eq. (65) is not yet ready to be an eigenvalue equation. The vector $|\varepsilon> \equiv \begin{pmatrix} \dot{\boldsymbol{\varepsilon}} \\ \boldsymbol{\varepsilon} \end{pmatrix}$ appears on the right side, but $\begin{pmatrix} \boldsymbol{\varepsilon} \\ \dot{\boldsymbol{\varepsilon}} \end{pmatrix}$ appears on the left. We need a 4×4 matrix Y that rearranges the latter vector into the former. Such a Y is easy to construct:

$$\begin{pmatrix} \dot{\varepsilon}_x \\ \dot{\varepsilon}_y \\ \varepsilon_x \\ \varepsilon_y \end{pmatrix} = \begin{pmatrix} 0 & 0 & 1 & 0 \\ 0 & 0 & 0 & 1 \\ 1 & 0 & 0 & 0 \\ 0 & 1 & 0 & 0 \end{pmatrix} \begin{pmatrix} \varepsilon_x \\ \varepsilon_y \\ \dot{\varepsilon}_x \\ \dot{\varepsilon}_y \end{pmatrix} \equiv Y|\varepsilon>. \quad (66)$$

With this we introduce the matrix $N = \Lambda Y$ to obtain

$$N = \begin{pmatrix} 0 & 2\omega & -\varphi_{\omega_{xx}} & -\varphi_{\omega_{yx}} \\ -2\omega & 0 & -\varphi_{\omega_{yx}} & -\varphi_{\omega_{yy}} \\ 1 & 0 & 0 & 0 \\ 0 & 1 & 0 & 0 \end{pmatrix}. \quad (67)$$

Equations (63) and (64) remain intact with N. Now we can require $|\varepsilon>$ to be an eigenvector of N. In other words, we require $N|\varepsilon> = \mu|\varepsilon>$, where $\mu = const$. Since $N|\varepsilon> = \frac{d|\varepsilon>}{dt}$,

$$|\varepsilon(t)> = e^{\mu t}|\varepsilon(0)>. \quad (68)$$

Any nontrivial solution requires $|N - \mu 1| = 0$, or

$$\begin{vmatrix} -\mu & 2\omega & -\varphi_{\omega_{xx}} & -\varphi_{\omega_{yx}} \\ -2\omega & -\mu & -\varphi_{\omega_{yx}} & -\varphi_{\omega_{yy}} \\ 1 & 0 & -\mu & 0 \\ 0 & 1 & 0 & -\mu \end{vmatrix} = 0. \quad (69)$$

Let us begin our eigenvalue quest with L4 and L5, for which $s_1 = s_2 = a$. Equations (48)–(50) are the second derivatives needed for L4 and L5. The determinant of Eq. (63) gives four roots,[12]

$$\mu = \pm\frac{i\omega}{2}\sqrt{2 \pm \sqrt{27\kappa^2 - 23}}, \quad (70)$$

where we recall that $\kappa = (m_1 - m_2)/M$.

It takes only one positive real eigenvalue to render a Lagrange point unstable, because any $\boldsymbol{\varepsilon}$ will in general be a superposition of all four eigenvectors, including any with a positive real eigenvalue, which by Eq. (68) renders the point unstable. Orbital motion—and thus relative stability—about L4 and L5 will result in cases where all the μ are imaginary, which requires $27\kappa^2 - 23 \geq 0$, or $\kappa \geq \sqrt{23/27} \approx 0.923$. This in turn requires $m_1 \geq 24.96 m_2$. When this is satisfied, then $2 - \sqrt{27\kappa^2 - 23} > 0$, and the i in Eq. (70) survives for all four eigenvalues. Thus a satellite displaced off of L4 or L5 can orbit the Lagrange point—orbiting a point in space!—if the heavier body's mass is at least about 25 times that of the smaller one. When this happens, asteroids orbiting L4 or L5 are called Trojans, after the three asteroids Agamemnon, Achilles, and Hector (names borrowed from Trojan War characters), the dominant rocks among some five thousand asteroids that orbit the Sun-Jupiter system's L4 and L5. In 2010 NASA's WISE telescope found the first Trojan asteroid at L4 in the Sun-Earth system.[13]

Turning to L1 for the Sun-Earth system, when we insert Eqs. (52) and (53) into Eq. (67) we find two real and two imaginary eigenvalues[14]:

$$\mu = \pm\sqrt[4]{30}\,\omega, \quad \pm i\sqrt[4]{30}\,\omega. \quad (71)$$

The positive real eigenvalue shows in Eq. (68) that a satellite that slips off of the Sun-Earth L1 will be driven away with a $1/e$ time of

$1/\mu \approx$ 23 days, where $\omega = 2\pi$ rad/yr. A satellite stationed at L1 requires frequent positional adjustments to remain near L1 for much longer than a couple of weeks.

By the same method, similar results hold for L2 and L3—they also have at least one positive real eigenvalue. The $1/e$ time for the Sun-Earth L2 is about the same as for L1, but for L3 the $1/e$ time is about 150 years. With L3 always on the side of the Sun opposite the Earth, science fiction writers have fun imagining a planet at L3 that diabolical aliens use as a base for an attack on Earth. Happily for Earth, the aliens would have to bring their own planet with them and park it at L3, because the time required for a planet to establish itself there by usual planet-building mechanisms comes up a bit short!

Enjoy and appreciate those marvelous JWST images!

References

7. These results agree with those of Neil J. Cornish in "The Lagrange Points," a document created for WMAP Education and Outreach, map.gsfc.nasa.gov/ContentMedia/lagrange.pdf.

8. Suggestions for the algebra: Let $\gamma \equiv \sqrt[3]{\alpha/3}$ in $s_1 = r_1 + x = a(1 + \alpha - \gamma)$ and $s_2 = r_2 - x = a(\beta - 1 + \gamma)$. Use $\beta \approx 1$, $m_1 \approx M$, and from Eq. (31) write $m_2 = \alpha M \approx \alpha m_1$. Where Cornish[7] obtains $\varphi_{\omega_{xx}} = -9\omega^2$, I obtain $-10\omega^2$; we agree on $\varphi_{\omega_{yy}}$ and $\varphi_{\omega_{xy}}$. Both are making approximations.

9. If a particle moves in N spatial dimensions, there are 2N phase-space coordinates, an instantaneous position coordinate and an instantaneous velocity coordinate, for each dimension. For example, a one-dimensional simple harmonic oscillator has energy $E = \frac{1}{2}mv^2 + \frac{1}{2}kx^2$. Dividing by the constant energy, this gives the equation of an ellipse in *x*-*v* space, $1 = \frac{mv^2}{2E} + \frac{kx^2}{2E}$. At any instant the state of the simple harmonic oscillator can be specified by its (x, v) coordinates on this ellipse. Canonical momentum coordinates rather than velocities are more typically used to map phase space, because (recalling Lagrangian and Hamiltonian mechanics) position and momentum are canonically conjugate variables.

10. For example, $\hat{\mathbf{i}}$, $\hat{\mathbf{j}}$, and $\hat{\mathbf{k}}$ form a basis for all vectors in *xyz* space.

11. For the invertible matrix theorem, see, e.g., David C. Lay, *Linear Algebra and Its Applications*, 3rd ed. (London: Pearson, 2006), pp. 129–130.

12. Because of the ubiquitous ω^2 in the second derivatives, I find it convenient to write $\mu \equiv \gamma\omega^2$ for some γ. Then Eq. (69) gives $\gamma^4\omega^4 + \gamma^2\omega^2 + (27/16)(1 - \kappa^2) = 0$. Setting $u = (\gamma\omega)^2$ offers a quadratic equation for u. Reversing back through the changes of variables gives Eq. (70). The eigenvalue μ, which is a frequency, gives the more rigorous version of the business with ω' in the lines below Eq. (55).

13. science.nasa.gov/resource/what-is-a-lagrange-point

14. Cornish[7] obtains for these eigenvalues $\mu = \pm\,\omega\sqrt{1 + 2\sqrt{7}} \approx \pm 2.508\omega$ and $\pm\, i\,\omega\sqrt{2\sqrt{7} - 1} \approx \pm 2.072\, i\omega$, whereas I obtain $\sqrt[4]{30} \approx 2.340$ as the real numerical coefficient in all four eigenvalues. My approximations are probably cruder than those of Cornish, who supplies few details of his intermediate steps. My purpose here is to illustrate *how* the Lagrange points are deduced, the logic that connects premise to conclusion, over obtaining precise values for the final results. For high precision, numerical methods are recommended. NASA needs high precision; a single satellite consumes the careers of many people.

Figure 5: *In this near-infrared JWST image, ionized hydrogen (cyan) wraps around an infrared-dark cloud while other clouds appear bright (pink). Credit: NASA, ESA, CSA, STScI, Samuel Crowe (UVA).*